Eur Biophys J (2010) 39:481–495
DOI 10.1007/s00249-009-0435-z

ORIGINAL PAPER

Hydrodynamic multibead modeling: problems, pitfalls, and solutions. 2. Proteins

Peter Zipper · Helmut Durchschlag

Received: 22 November 2008 / Revised: 23 February 2009 / Accepted: 28 February 2009 / Published online: 24 March 2009

Abstract Hydrodynamic models of proteins have been generated by recourse to crystallographic data and applying a filling model strategy in order to predict both hydrodynamic and scattering parameters. The design of accurate protein models retaining the majority of the molecule peculiarities requires usage of many beads and consideration of many serious problems. Applying the expertise obtained with ellipsoid models and pilot tests on proteins, we succeeded in constructing precise models for several anhydrous and hydrated proteins of different shape, size, and complexity. The models constructed consist of many beads (up to about 11,000) for the protein constituents (atoms, amino acid residues, groups) and preferentially bound water molecules. While in the case of small proteins, parameter predictions are straightforward, computations for giant proteins necessitate drastic reductions of the number of initially available beads. Among several auxiliary programs, our advanced hydration programs, HYDCRYST and HYDMODEL, and modified versions of García de la Torre's program HYDRO were successfully employed. This allowed the generation of realistic protein models by imaging details of their fine structure and enabled the prediction of reliable molecular parameters including intrinsic viscosities. The appearance of the models and the agreement of molecular properties and distance distribution functions $p(r)$ of unreduced and reduced models can be used for a meticulous inspection of the data obtained.

Keywords Multibead modeling · Data reduction · Anhydrous and hydrated proteins · Parameter predictions · Hydrodynamics

Introduction

The present knowledge of proteins includes information about their amino acid (AA) sequence and precise 3D structure (Creighton 1993; Serdyuk et al. 2007). Currently, crystallographically analyzed proteins span a wide range of simple and complex molecules of quite different shape and mass, investigated in the absence or presence of various ligands. The solution properties of many proteins have also been investigated by hydrodynamic and scattering techniques. Besides the experimental characterization of proteins in terms of hydrodynamic and scattering molecular parameters, bead modeling approaches were successful in predicting properly various molecular quantities (Carrasco and García de la Torre 1999; García de la Torre et al. 2000; Zipper et al. 2005; Byron 2008).

A short outline of the applied hydrodynamic modeling strategies in context with concurrent hydrodynamic and scattering calculations has been given in Part 1. The programs usually to be used for predicting hydrodynamic properties of bead models comprise the freely available programs HYDRO (García de la Torre et al. 1994), HYDRO++ (García de la Torre et al. 2007), and

AUC&HYDRO 2008—Contributions from 17th International Symposium on Analytical Ultracentrifugation and Hydrodynamics, Newcastle, UK, 11–12 September 2008.

P. Zipper
Physical Chemistry, Institute of Chemistry, University of Graz, Heinrichstrasse 28, 8010 Graz, Austria

H. Durchschlag (✉)
Institute of Biophysics and Physical Biochemistry, University of Regensburg, Universitätsstrasse 31, 93040 Regensburg, Germany
e-mail: helmut.durchschlag@biologie.uni-regensburg.de

HYDROPRO (García de la Torre et al. 2000), amongst other programs for special purposes. The HYDROPRO approach uses a shell model and can be used if only hydrodynamic data are wanted, whereas HYDRO and HYDRO ++ exploit 'filling model' strategies, preferably to be adopted if both hydrodynamic and scattering parameters are desired.

In the case of proteins, recourse to high-resolution crystallographic data allows the atomic coordinates of all constituents (AAs, ligands) to be used. Owing to the wide spectrum of size and complexity of proteins (molar masses ranging from a few up to several thousand kg/mol), hydrodynamic modeling has to be able to handle not only a few hundred but even a myriad of atoms or atomic groups and a variety of special problems. Among the problems to be addressed, the often immense number (N) of unequally sized and overlapping beads, requirement of reduction approaches, and the choice of an appropriate volume correction turned out to be the most serious ones (Zipper et al. 2005; Zipper and Durchschlag 2007b). In the course of our recent investigations, the maximum number of beads (N_{max}) to be feasible for hydrodynamic modeling and the applicability of the reduced volume correction (RVC) to anisometric particles turned out to be burning issues. As a first step in this direction, a variety of model calculations on two- and three-axial model ellipsoids of different axial ratios were performed (Part 1). In this study, we extended our knowledge by performing model calculations on real molecules, namely proteins exhibiting quite different molecular features, applying primarily the programs by the García de la Torre group (HYDRO, HYDRO++) and our own in-house programs. In this context, however, it should be mentioned that in the past several other approaches have been developed to handle the construction of hydrodynamic bead models with reduced numbers of beads [e.g. the freely available programs AtoB (Byron 1997) and SOMO (Rai et al. 2005)] and to allow the generation of bead models for scattering purposes (Glatter 1980; Durchschlag et al. 1991; Svergun et al. 1995). These approaches may also be used in conjunction with disposable atomic coordinates.

Methods

Proteins

Atomic coordinates and masses of the proteins analyzed were taken from the Protein Data Bank PDB (Berman et al. 2000) and/or the SWISS-PROT protein knowledge base (Boeckmann et al. 2003). The proteins under investigation comprise: (1) pig insulin (PDB accession code: 4INS; SWISS-PROT entry: P01315); (2) bovine pancreatic trypsin inhibitor (4PTI; P00974); (3) bovine pancreatic ribonuclease A (1RBX; P61823); (4) hen egg white lysozyme (2LYZ; P00698); (5) *E. coli* malate synthase G (molecules A and B: 1P7T; P37330); (6) bacteriophage fr capsid (1FRS; P03614); and (7) hexagonal bilayer (HBL) complex of *Lumbricus terrestris* hemoglobin (heme-liganded globin chains A−L plus heme-deficient linker chains M−O: 2GTL; P13579 (A,E,I), P02218 (B,F,J), P11069 (C,G,K), O61233 (D,H,L), Q9GV76 (M), Q2I743 (N), Q2I742 (O); for further details see Durchschlag et al. 2007; Durchschlag and Zipper 2008). All protein models were visualized by the program RASMOL (Sayle and Milner-White 1995).

Calculation of parameters of anhydrous protein models

The number of beads, N, for hydrodynamic modeling of the anhydrous small proteins insulin (4INS), pancreatic trypsin inhibitor (4PTI), ribonuclease A (1RBX), and lysozyme (2LYZ) was chosen to be identical to the number of respective atoms given in the PDB file (there is no need for bead reduction in the case of small N values). In the case of the medium-sized malate synthase G (1P7T) either the available atoms or the AA residues (after reducing the original value of N) were used. For the huge, 180-meric proteins, the phage capsid (1FRS) and the *L.t.* HBL complex (2GTL), only reduced models could be applied.

The molecular volumes, V, of the protein models can be calculated by summing up the volumes of the individual constituents (beads) by the Traube procedure as outlined previously (Durchschlag and Zipper 2005, 2008; Zipper and Durchschlag 2007b). The obtained volumes are anhydrous volumes.

The radius of gyration, R_G, and the pair-distance distribution function, $p(r)$, of the protein models were calculated from the radii and coordinates of the constituent beads (Glatter 1980; Glatter and Kratky 1982) and the bead volume as statistical weight. This conforms to the usage in hydrodynamic calculations, whereas for comparisons with experimental scattering data the electron or scattering length densities would have to be included in the calculation of R_G and $p(r)$.

Translational diffusion coefficient, D, sedimentation coefficient, s, and intrinsic viscosity, $[\eta]$, were computed by means of our modified versions of HYDRO (García de la Torre et al. 1994) or by HYDRO++ (García de la Torre et al. 2007), taking into account the pitfalls and precautions mentioned in Part 1. For comparing the available approaches for the computation of $[\eta]$, again, several procedures were tested: no volume correction (NVC), full volume correction (FVC), adjusted volume correction (AVC), cubic substitution (CBS), and our reduced volume correction (RVC).

In the context of the FVC and RVC approaches, the different ways to calculate $[\eta]$ should be mentioned explicitly:

$$[\eta]_{\mathrm{FVC}} = [\eta]_{\mathrm{NVC}} + \frac{2.5\,N_{\mathrm{A}}V}{M}$$

$$[\eta]_{\mathrm{RVC}} = [\eta]_{\mathrm{NVC}} + \frac{2.5\,N_{\mathrm{A}}V}{N^{1/3}M}$$

where N_{A} is Avogadro's number, and N, V, and M denote number, total volume and mass of the beads, respectively. Thus, a simple analytical expression may be given to derive $[\eta]_{\mathrm{RVC}}$ from $[\eta]_{\mathrm{FVC}}$:

$$[\eta]_{\mathrm{RVC}} = [\eta]_{\mathrm{FVC}} - \frac{2.5\,N_{\mathrm{A}}V}{M}\left(\frac{N^{1/3}-1}{N^{1/3}}\right)$$

Since the values for $[\eta]_{\mathrm{FVC}}$ can be obtained by original versions of HYDRO or by HYDRO++ (option ICASE = 11), $[\eta]_{\mathrm{RVC}}$ can be gained simply by an algebraic transformation. By contrast, calculation of the values for $[\eta]_{\mathrm{AVC}}$ and $[\eta]_{\mathrm{CBS}}$ requires application of HYDRO++. In the case of extensive bead numbers, N, however, modified versions of HYDRO are needed to assess the values for $[\eta]$ (cf. Part 1): models with $N > 20{,}000$ (NVC, FVC, RVC); models with $N > 250$ (CBS); no modified approach of HYDRO++ for AVC is available. Similarly, calculations in the double precision mode require adaptations of the existing program HYDRO.

Calculation of parameters of hydrated protein models

To predict the features of hydrated protein models, the water molecules bound preferentially to the protein surface have to be taken into account. This can be realized by assuming a water shell, by blowing up protein constituents to some extent, or by applying special hydration algorithms. To obtain biophysically realistic protein–water models, we proceeded by calculating the exact protein surface analytically by the program SIMS (Vorobjev and Hermans 1997) and then adopted our advanced hydration algorithms HYDCRYST or HYDMODEL (Durchschlag and Zipper 2002, 2005, 2008) based on the hydration numbers for individual AA residues (Kuntz 1971).

Our in-house hydration programs are based on the initial atomic coordinates of the protein (HYDCRYST) or on the AA coordinates of a reduced model derived therefrom (HYDMODEL). The programs select preferential positions for bound water molecules (N_{w}); the selected waters, assigned to the accessible AA residues, were then attached to the anhydrous (dry) protein models. A fine-tuning of the extent of hydration can be achieved by a scaling factor, f_{K}, acting on the hydration numbers. Of course, the number of beads to be applied for hydrodynamic modeling, N, is composed of the beads of the protein moiety and the water beads. If N exceeds N_{max}, alternative modes of modeling the hydrated proteins have to be considered for hydrodynamic calculations. As long as the number of beads representing the protein moiety does not exceed N_{max}, one can use the approach of expanding the beads on the surface according to the volume of water molecules assigned to them. This approach is also implemented in our programs HYDCRYST and HYDMODEL and is executed together with the usual hydration routine. In the case of large proteins, however, if already the hydrodynamic modeling of the anhydrous state requires the application of reduction procedures, the hydrated models obtained by HYDCRYST or HYDMODEL have to be reduced by mapping the protein and water beads onto grids of appropriate symmetry and voxel size (VS).

Results and discussion

In the following, models of anhydrous and hydrated proteins were constructed, applying the information from crystallographic, sequence and hydration databases. The proteins applied cover a wide range of masses and complexity: 6–3,367 kg/mol, 1–180 subunits, presence of heteroatoms (Zn in the case of insulin; heme groups in the HBL complex of *L.t.* hemoglobin), and numerous missing AA residues in some regions of the HBL complex.

Models of anhydrous proteins and of protein-water complexes are displayed in Figs. 1, 2, and 3 in space-filling format. Quantitative results of the proteins under consideration in terms of molecular parameters are listed in Tables 1 and 2, together with many details of the underlying calculations.

The simple proteins analyzed (insulin, pancreatic trypsin inhibitor, ribonuclease A, lysozyme and malate synthase G) exhibit differences with respect to shape and distribution of bound water molecules (protein constituents shown in *CPK colors* and waters in *cyan*) (Fig. 1). The models obtained for malate synthase G (1P7T) were obtained on the basis of the coordinates of atoms or constituent AA residues, with nearly identical structural features.

The capsid of the bacteriophage fr is a huge and complex protein, composed of 60 copies of a building block consisting of three chemically identical subunits (Fig. 2). In accord with previous findings (Zipper and Durchschlag 2007a, b), different reduction approaches rendered reliable models. Running mean (RM) reductions of the crystal structure of each subunit (1FRS), using different bead diameters (BD) or compression indices (ICOM), gave similar anhydrous models, irrespective of the use of atomic

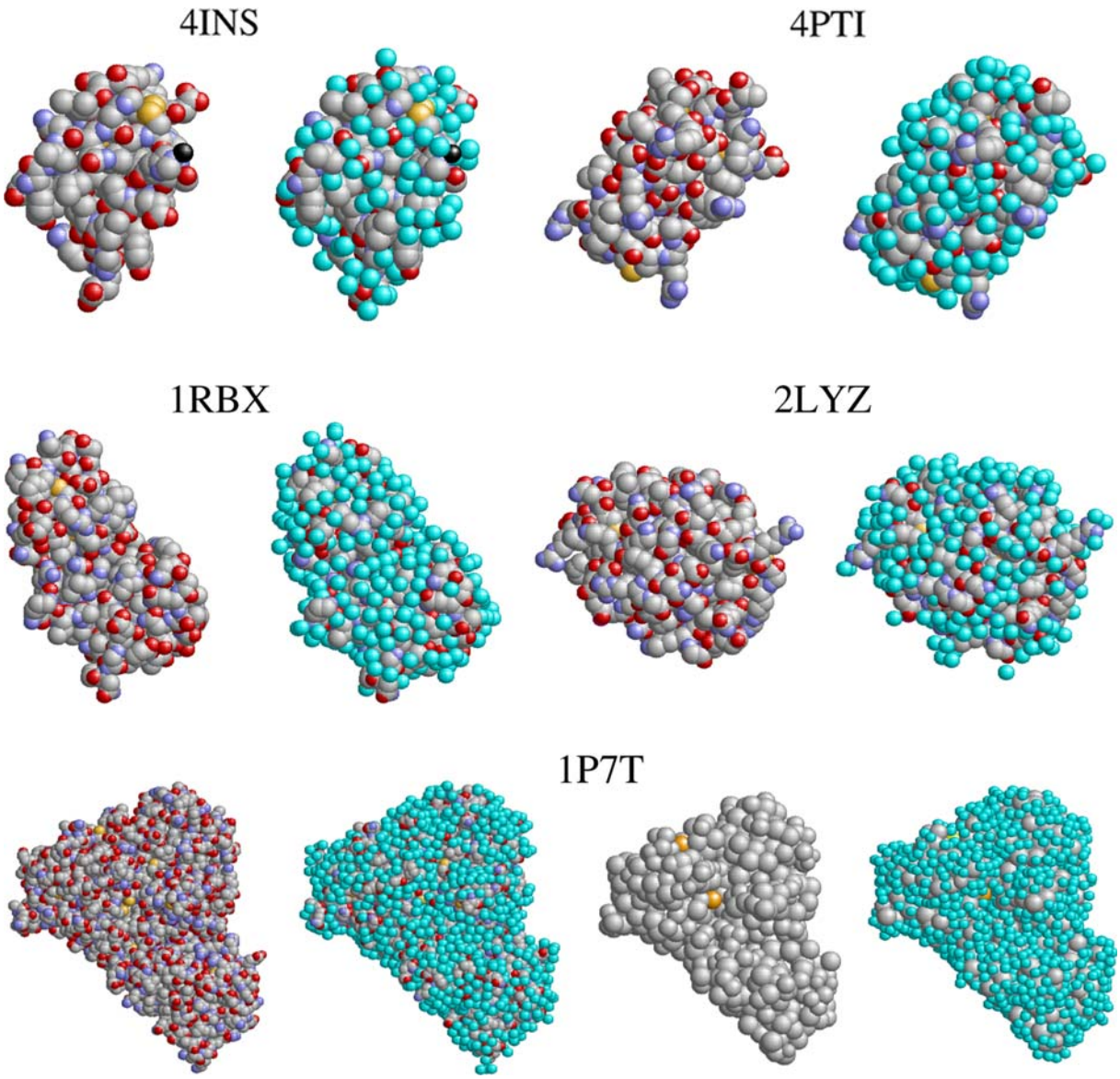

Fig. 1 Space-filling models for selected anhydrous and hydrated proteins based on their crystallographic data: insulin (*4INS*), pancreatic trypsin inhibitor (*4PTI*), ribonuclease A (*1RBX*), lysozyme (*2LYZ*), and malate synthase (*1P7T*, molecule A). The basic protein atoms are shown in the usual CPK colors (C in *light gray*, O in *red*, N in *light blue*, and S in *yellow*); Zn (*4INS*) is highlighted in *black*. The model for *1P7T* is also shown in AA residues representation (displayed in *gray*; two residues representing cystein and S-hydroxy-cystein are displayed in *orange*). Bound water molecules are displayed in *cyan*. All hydrated models were generated with $f_K = 1.0$; for further details of hydration, see Table 1

coordinates or AA residues (panels a and b). The reduction process, however, should not exceed a factor of about 100, to guarantee preservation of structural features. Application of hexagonal grid (HG) approaches of different voxel size (VS), placing the resulting beads at local centers of gravity, were equally successful (panel c). It has to be mentioned that the only feasible reduction procedure for models of hydrated capsids is the HG approach. The inclusion of the bound waters in the reduction process mainly enhances the bead numbers N as compared to the HG-reduced anhydrous models, thereby obscuring the role of the voxel size for the reduction of the protein moiety itself.

Modeling the structure of the giant HBL complex of *L.t.* hemoglobin turned out to be a rather sophisticated problem (Fig. 3). Owing to numerous missing AA residues in the linker chains, the anhydrous and hydrated models of the original HBL complex revealed a structure with a too big cavity in the central core of the complex (panel a). By

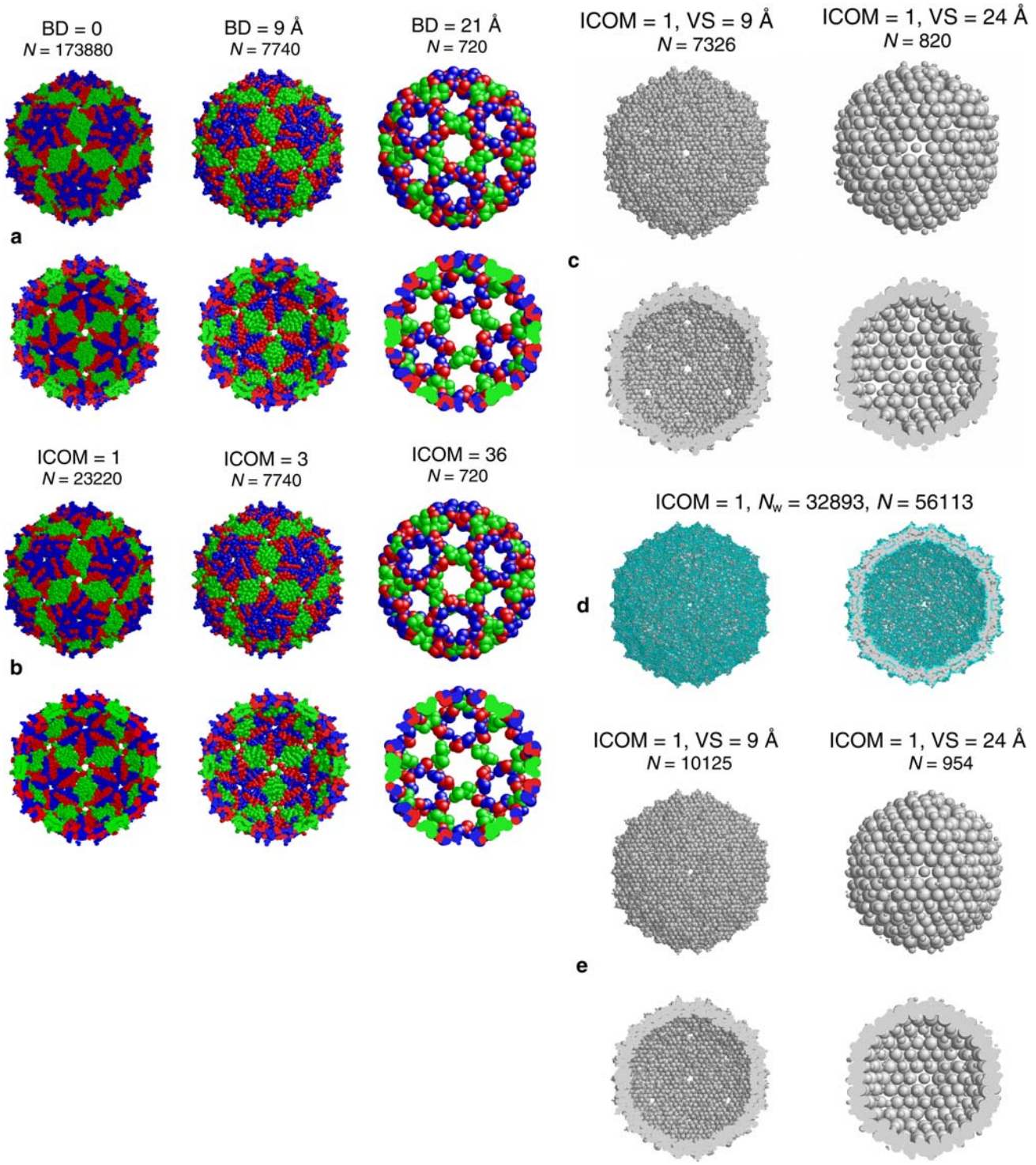

Fig. 2 Bead models for the capsid of bacteriophage fr, based on the crystal structure 1FRS of the trimeric building block (subunits A, B, and C, displayed in *red*, *blue*, and *green*, respectively). Panels **a** and **b** show the models (together with the corresponding slabs) obtained by applying RM reductions separately to each subunit of the building block, using different bead diameters BD (**a**) or compression indices ICOM (**b**), followed by application of the appropriate symmetry relations. The models obtained with BD = 0 or ICOM = 1 correspond to the original crystal structure in atomic coordinates (**a**) or to the AA representation (**b**) of the capsid. The reduced models and the slabs shown in **c** were generated by mapping the AA representation of the entire anhydrous capsid into hexagonal grids of different voxel size *VS*, placing the resulting beads at local centers of gravity. Panel **d** shows the AA representation of the hydrated capsid (hydration with $f_K = 1.0$) together with the corresponding slab (AA residues are displayed in *gray* and waters in *cyan*), and panel **e** presents two reduced models (and their slabs) obtained by mapping the hydrated capsid (**d**) into hexagonal grids of different VS

contrast, constructing a HBL model with the aid of extra beads, acting as substitutes for the missing AA residues, yielded a model (panel b) in agreement with experimental parameters (Durchschlag et al. 2007). For the purpose of hydration, hypothetical hydration numbers were assigned to the extra beads; these were obtained by summing up the hydration numbers of the missing AA residues. An inspection of a hypothetical HBL complex, built from models of the subunits without linker chains, discloses a structure more hollow than the original HBL complex (panel c).

In addition to the rather superficial examination of the models, a wide selection of computations with all proteins under analysis has been performed (Table 1). Both structural and hydrodynamic parameter calculations by means of HYDRO and HYDRO++ (if applicable) for anhydrous and hydrated protein models were executed. HYDRO was run preferably in double-precision mode. An analysis of the data obtained reveals that all parameter predictions for R_G, D (and thus s), and $[\eta]$ were successful. In accord with the findings for various ellipsoid models (Part 1), the viscosity calculations by the CBS and RVC approaches were highly efficient and yielded similar results, slightly higher than the values for NVC, but significantly lower than the AVC approach and, in particular, the FVC case. Due to the restrictions in N_{max}, however, calculations applying CBS are restricted to low N numbers. As expected, the results for the hydrated models show that the number of beads, N, to be used for the predictions of the hydrated models increases as compared to the anhydrous models. A fine-tuning of the extent of hydration by varying scaling factors ($0.8 < f_K < 7.0$) leads to slightly different values for R_G, D and $[\eta]$, depending on the extent of hydration. Selecting a factor of $f_K = 1.0$, the tabulated values of N_w for the protein models correspond to hydrations ranging from $\delta_1 = 0.240$ g/g (1FRS) to $\delta_1 = 0.346$ g/g (4PTI); averaging the hydrations obtained with $f_K = 1.0$ leads to $\delta_1 = (0.29 \pm 0.03)$ g/g. As may be taken from the example malate synthase G (1P7T), the parameter predictions for original and reduced models gave similar results, both for the molecule A and the molecule B.

While calculations with the small- and medium-sized proteins did not pose problems, parameter computations of the giant proteins raised various serious difficulties to be overcome, mainly in context with the enormous number of coordinates of the original models (Table 1). However, after appropriate data reductions by means of RM or HG approaches and variation of the required input parameters (BD, ICOM, and VS), the problems can be solved satisfactorily. Also in the case of these huge entities, parameter predictions for both anhydrous and hydrated models are reliable. This is proven for the phage capsid (1FRS), but also for the original, modified and hypothetical HBL complexes of *L.t.* hemoglobin (2GTL).

Fig. 3 *Top* and *side* views together with slabs of models of ▶ anhydrous and hydrated HBL complexes of *L.t.* hemoglobin based on the crystal structure 2GTL. The models of the anhydrous complexes (AA residues are displayed in *gray*, heme groups in *black*) are shown in the *first two columns* on the *left*; the additional large beads in the model of the modified complex represent the AA residues missing in the original crystal structure at the N (*blue*) and C (*red*) termini of the linker chains. The successive two columns present the unreduced models of the complexes hydrated by means of HYDMODEL (waters are displayed in *cyan*; for details of hydration see Table 1). The rightmost column presents reduced models (displayed in *gray*) of the hydrated complexes (voxel size = 11.0 Å, for the hypothetical complex 10.0 Å)

A quantification of the mean ratios of viscosities in terms of $\langle[\eta]_x/[\eta]_{RVC}\rangle$ quotients yields results (Table 2) which verify the conclusions drawn on the viscosity predictions mentioned previously. The ratio $\langle[\eta]_{CBS}/[\eta]_{RVC}\rangle$ is close to unity, the ratio $\langle[\eta]_{NVC}/[\eta]_{RVC}\rangle$ slightly lower, and the $\langle[\eta]_{AVC}/[\eta]_{RVC}\rangle$ value slightly greater, whereas the values for $\langle[\eta]_{FVC}/[\eta]_{RVC}\rangle$ exceed unity by far. This obviously means that, in the case of proteins composed of many beads, FVC fails, whereas an appropriate volume correction or no correction is much more purposive.

A comparison of the distance distribution functions, $p(r)$, of the various models for the proteins analyzed (Fig. 4) displays pronounced differences in the profiles. Owing to the different shape and extension of the particles, of course, the shape of the profiles and the maximum particle diameters must differ. All small- and medium-sized proteins reveal pronounced differences between anhydrous and hydrated models (panels a and b), caused by the water sheet of the protein. Huge protein particles such as the HBL complex of *L.t.* hemoglobin (panel c) are not significantly influenced by a water layer as follows from the almost perfect coincidence of the profiles for the protein and the protein-water complexes, respectively. For obvious reasons, the profiles between original and modified HBL complexes differ slightly, while the profiles of these complexes and the profile of the hypothetical complex built from the subunits without linkers disagree. Of course, this discrepancy is caused by the lacking mass in the core of the hypothetical complex.

The overall appearance of the $p(r)$ function of the capsid of the bacteriophage fr (Fig. 5) differs strikingly from those of the proteins discussed above. This is due to the differences in the mass distribution within these proteins. While the structure of the capsid resembles a hollow sphere, the other proteins are more or less solid particles. Consequently, the mass distribution reflected by the $p(r)$ functions must differ. The $p(r)$ profile of the capsid is characterized by a sharp maximum located at large r values

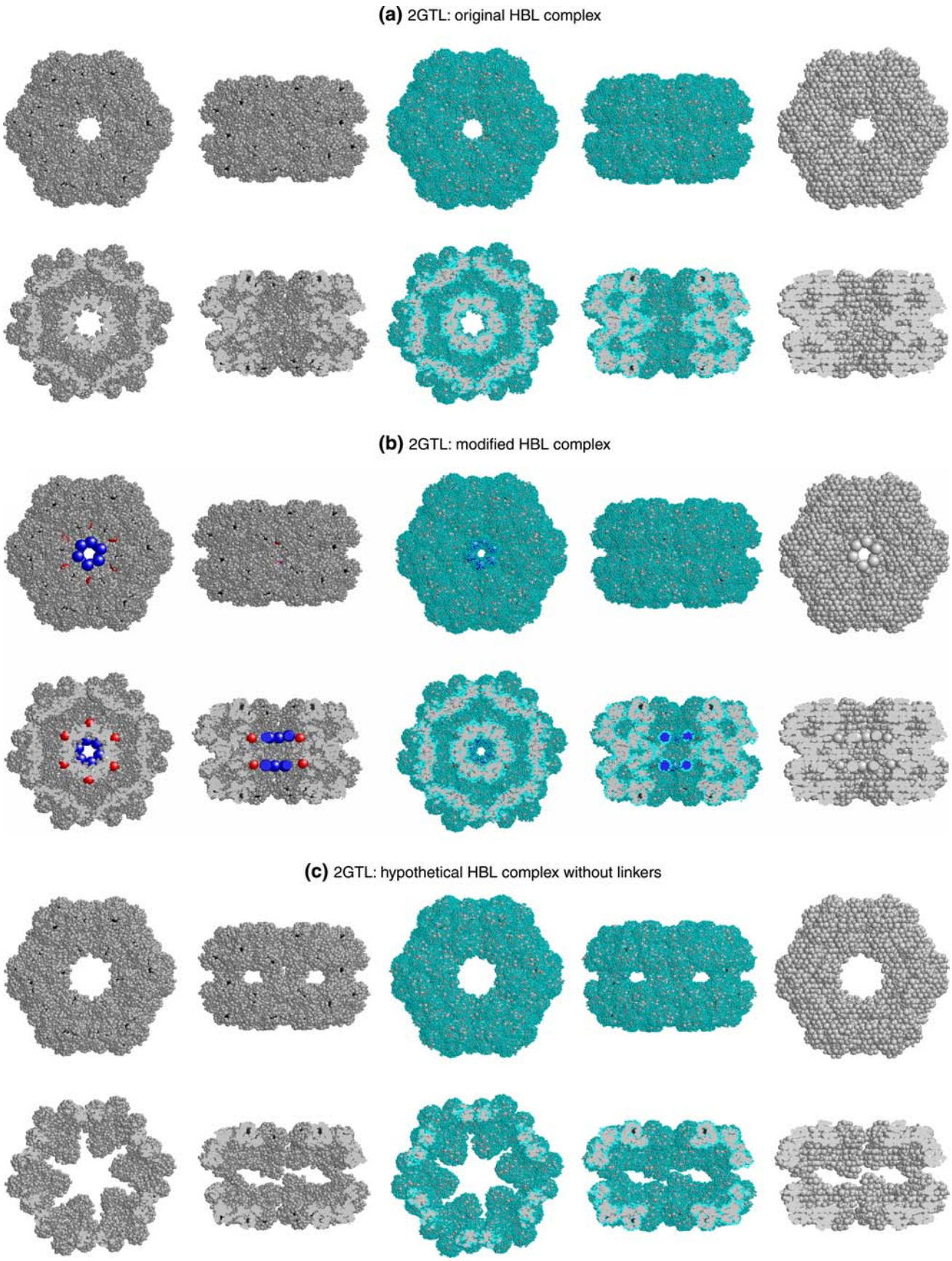
(a) 2GTL: original HBL complex
(b) 2GTL: modified HBL complex
(c) 2GTL: hypothetical HBL complex without linkers

Table 1 Structural and hydrodynamic parameters of anhydrous and hydrated protein models, computed by means of HYDRO (if possible in double-precision mode) and HYDRO++

Protein	f_K	N_w	N	V (Å^3)	R_G (Å)	$D \times 10^7$ (cm^2/s)	$[\eta]_{NVC}$ (cm^3/g)	$[\eta]_{FVC}$ (cm^3/g)	$[\eta]_{RVC}$ (cm^3/g)	$[\eta]_{CBS}$ (cm^3/g)	$[\eta]^a_{AVC}$ (cm^3/g)
4INS (chains A, B), anhydrous[b]		0	404	6957	10.27	16.44	2.335	4.128	2.578	2.550	2.828
−, hydrated[c]	0.8	91	495	9178	10.95	14.97	3.111	5.476	3.410	3.372	3.549
	0.9	102	506	9446	11.03	14.85	3.189	5.623	3.494	3.456	3.667
	1.0	108	512	9593	11.12	14.77	3.239	5.711	3.548	3.518	3.765
	1.5	152	556	10666	11.46	14.17	3.683	6.432	4.017	3.990	4.376
	2.0	175	579	11227	11.73	13.90	3.903	6.797	4.250	4.238	4.625
4PTI, anhydrous[d]		0	454	7781	11.03	15.72	2.418	4.216	2.652	2.639	2.953
−, hydrated[c]	0.8	100	554	10221	11.71	14.33	3.207	5.568	3.494	3.471	3.832
	0.9	114	568	10563	11.81	14.22	3.284	5.724	3.578	3.555	3.926
	1.0	125	579	10831	11.95	14.01	3.431	5.933	3.731	3.708	4.115
	1.5	178	632	12125	12.28	13.47	3.856	6.757	4.183	4.162	4.597
	2.0	202	656	12710	12.45	13.20	4.099	7.036	4.437	4.423	4.888
1RBX, anhydrous[e]		0	951	16110	14.29	12.21	2.461	4.233	2.641	2.638	2.923
−, hydrated[f]	0.8	215	1166	21915	15.23	10.96	3.407	5.818	3.636	3.606[g]	4.019
	1.0	245	1196	22726	15.36	10.86	3.512	6.012	3.748	3.718[g]	4.175
	1.2	257	1208	23050	15.41	10.83	3.542	6.077	3.780	3.752[g]	4.225
	1.5	310	1261	24490	15.66	10.65	3.722	6.414	3.971	3.938[g]	4.458
2LYZ, anhydrous[h]		0	1001	16953	13.86	12.27	2.335	4.118	2.513	2.481[g]	2.880
−, hydrated[i]	0.80	198	1199	22041	14.77	10.99	3.246	5.565	3.465	3.426[g]	3.941
	1.00	225	1226	22735	14.93	10.84	3.383	5.775	3.607	3.571[g]	4.110
	1.25	272	1273	23943	15.17	10.66	3.558	6.077	3.790	3.756[g]	4.322
	1.50	303	1304	24739	15.35	10.59	3.638	6.240	3.876	3.847[g]	4.446
	1.75	329	1330	25408	15.43	10.54	3.679	6.362	3.932	3.904[g]	4.526
	2.00	340	1341	25691	15.50	10.51	3.731	6.434	3.976	3.946[g]	4.590
1P7T (mol. A), anhydrous[j]		0	5414	93420	26.08	6.530	2.855	4.682	2.959		
−, hydrated[c]	1.0	1110	6524	120504	27.31	6.099	3.520	5.878	3.646		
	2.0	1509	6923	130240	27.76	5.986	3.725	6.273	3.859		
	3.0	1691	7105	134681	27.97	5.934	3.825	6.460	3.962		
	4.0	1770	7184	136609	28.06	5.915	3.860	6.533	3.999		
	5.0	1803	7217	137414	28.11	5.905	3.882	6.570	4.021		
	6.0	1814	7228	137682	28.12	5.902	3.887	6.581	4.027		
	7.0	1822	7236	137878	28.13	5.901	3.890	6.588	4.030		
1P7T (mol. B), anhydrous[k]		0	5358	92442	25.81	6.574	2.829	4.657	2.934		

Table 1 continued

Protein	f_K	N_w	N	V (Å^3)	R_G (Å)	$D \times 10^7$ (cm^2/s)	$[\eta]_{NVC}$ (cm^3/g)	$[\eta]_{FVC}$ (cm^3/g)	$[\eta]_{RVC}$ (cm^3/g)	$[\eta]_{CBS}$ (cm^3/g)	$[\eta]^a_{AVC}$ (cm^3/g)
−, hydrated[c]	1.0	1149	6507	120478	27.11	6.133	3.499	5.882	3.627		
	2.0	1547	6905	130190	27.55	6.013	3.716	6.291	3.851		
	3.0	1729	7087	134631	27.74	5.964	3.809	6.472	3.948		
	4.0	1802	7160	136412	27.83	5.951	3.836	6.534	3.976		
	5.0	1832	7190	147144	27.88	5.942	3.852	6.565	3.993		
	6.0	1840	7198	137339	27.88	5.941	3.855	6.571	3.995		
	7.0	1844	7202	137437	27.89	5.940	3.857	6.576	3.998		
1P7T (mol. A), reduced, anhydrous[l]		0	706	95327	26.18	6.589	2.779	4.643	2.988	2.995	3.242
−, hydrated[m]	1.0	1135	1841	123021	27.42	6.070	3.571	5.978	3.768		4.491
	2.0	1483	2189	131513	27.78	5.988	3.723	6.296	3.921		
	3.0	1610	2316	134612	27.91	5.963	3.769	6.403	3.968		
	4.0	1651	2357	135612	27.99	5.950	3.794	6.447	3.994		
	5.0	1671	2377	136100	28.03	5.946	3.803	6.465	4.002		
	6.0	1677	2383	136246	28.03	5.944	3.805	6.471	4.005		
	7.0	1679	2385	136295	28.04	5.944	3.806	6.472	4.005		
1P7T (mol. B), reduced, anhydrous[n]		0	705	95120	26.08	6.625	2.763	4.645	2.975	2.985	3.236
−, hydrated[m]	1.0	1152	1857	123229	27.29	6.092	3.569	6.006	3.767		4.502
	2.0	1501	2206	131745	27.68	6.016	3.711	6.316	3.911		
	3.0	1633	2338	134966	27.82	5.993	3.755	6.424	3.956		
	4.0	1678	2383	136064	27.87	5.982	3.776	6.467	3.977		
	5.0	1697	2402	136528	27.90	5.977	3.784	6.485	3.986		
	6.0	1708	2413	136796	27.91	5.977	3.786	6.492	3.988		
	7.0	1712	2417	136894	27.91	5.976	3.788	6.495	3.989		
1FRS, anhydrous, original[o]		0	173880		121.77						
−, reduced, BD = 9 Å[p]			7740	2996682	121.81	1.746[g]	5.906[g]	7.732[g]	5.999[g]		
			7722[q]	2992453	121.81	1.608	6.035	7.857	6.127		
−, reduced, BD = 12 Å[p]			3420	2996684	121.80	1.627	5.827	7.652	5.948		
−, reduced, BD = 15 Å[p]			1800	2996682	121.59	1.646	5.631	7.456	5.781		7.798
−, reduced, BD = 18 Å[p]			1080	2996682	121.28	1.650	5.580	7.405	5.757	5.839[g]	5.894
−, reduced, BD = 21 Å[p]			720	2996695	121.19	1.677	5.310	7.135	5.513	5.665	5.644
−, reduced, BD = 24 Å[p]			540	2996680	121.15	1.708	5.034	6.859	5.258	5.458	5.337
−, reduced, ICOM = 1[r,s]			23220		121.78						
−, reduced, ICOM = 3[r]			7740	2996684	121.78	1.735[g]	5.969[g]	7.795[g]	6.062[g]		
			7722[q]	2988960	121.79	1.602	6.093	7.913	6.185		
−, reduced, ICOM = 6[r]			3960	2996684	121.75	1.615	5.953	7.778	6.069		
−, reduced, ICOM = 9[r]			2700	2996684	121.70	1.614	5.963	7.788	6.094		
−, reduced, ICOM = 12[r]			1980	2996685	121.62	1.649	5.604	7.429	5.749		7.409

Table 1 continued

Protein	f_K	N_w	N	V (Å^3)	R_G (Å)	$D \times 10^7$ (cm^2/s)	$[\eta]_{NYC}$ (cm^3/g)	$[\eta]_{FYC}$ (cm^3/g)	$[\eta]_{RYC}$ (cm^3/g)	$[\eta]_{CBS}$ (cm^3/g)	$[\eta]^a_{AYC}$ (cm^3/g)
−, reduced, ICOM = 18[r]			1440	2996684	121.40	1.637	5.712	7.537	5.874		6.215
−, reduced, ICOM = 24[r]			1080	2996683	121.22	1.648	5.590	7.415	5.768	5.859[g]	5.914
−, reduced, ICOM = 36[r]			720	2996711	121.13	1.675	5.326	7.151	5.529	5.677	5.656
−, reduced, ICOM = 48[r]			540	2996691	121.20	1.677	5.313	7.136	5.537	5.691	5.643
−, reduced, VS = 9 Å[t]			7326	2996716	121.79	1.602	6.098	7.923	6.192		
−, reduced, VS = 12 Å[t]			3809	2996716	121.77	1.604	6.075	7.900	6.192		
−, reduced, VS = 15 Å[t]			2337	2996716	121.75	1.609	6.021	7.846	6.158		
−, reduced, VS = 18 Å[t]			1522	2996716	121.72	1.617	5.940	7.766	6.099		7.491
−, reduced, VS = 21 Å[t]			1062	2996717	121.68	1.624	5.861	7.686	6.040	6.058[g]	6.498
−, reduced, VS = 24 Å[t]			820	2996716	121.64	1.625	5.846	7.671	6.041	6.126	6.336
1FRS, hydrated[s,u]	1.0	32893	56113		122.09						
−, reduced, VS = 9 Å[v]			10125	3797911	122.06	1.696[g]	6.271[g]	8.584[g]	6.378[g]		
−, reduced, VS = 12 Å[v]			5007	3797912	122.05	1.583	6.326	8.639	6.461		
−, reduced, VS = 15 Å[v]			2885	3797910	122.03	1.587	6.279	8.592	6.441		
−, reduced, VS = 18 Å[v]			1887	3797909	122.00	1.592	6.221	8.534	6.408		8.901
−, reduced, VS = 21 Å[v]			1316	3797908	121.97	1.596	6.172	8.485	6.383	6.332[g]	7.403
−, reduced, VS = 24 Å[v]			954	3797910	121.93	1.602	6.111	8.425	6.346	6.344[g]	6.757
2GTL, original, anhydrous[w]		0	28884	4056130	107.80						
−, reduced, VS = 10.5 Å[x]			6939	4056196	107.78	1.637	4.180	5.994	4.275		
−, reduced, VS = 11.0 Å[x]			6222	4056195	107.78	1.638	4.170	5.984	4.269		
−, reduced, VS = 11.5 Å[x]			5595	4056196	107.77	1.641	4.151	5.965	4.254		
2GTL, original, hydrated[y]	1.0	52206	81090	5335180	107.96						
−, reduced, VS = 10.5 Å[z]			9072	5336917	107.95	1.663[g]	4.377[g]	6.764[g]	4.492[g]		
−, reduced, VS = 11.0 Å[z]			8094	5336917	107.94	1.657[g]	4.379[g]	6.765[g]	4.498[g]		
−, reduced, VS = 11.5 Å[z]			7212	5336917	107.94	1.609	4.404	6.791	4.528		
2GTL, modified, anhydrous[#]		0	28908	4150910	106.76						
−, reduced, VS = 10.5 Å[x]			6958	4150973	106.75	1.637	4.082	5.894	4.177		
−, reduced, VS = 11.0 Å[x]			6246	4150973	106.75	1.638	4.072	5.884	4.170		
−, reduced, VS = 11.5 Å[x]			5616	4150973	106.74	1.641	4.054	5.866	4.156		
2GTL, modified, hydrated[y]	1.0	54039	82947	5474860	106.83						
−, reduced, VS = 10.5 Å[z]			9275	5474421	106.82	1.672[g]	4.272[g]	6.663[g]	4.386[g]		
−, reduced, VS = 11.0 Å[z]			8239	5474421	106.82	1.664[g]	4.275[g]	6.665[g]	4.393[g]		
−, reduced, VS = 11.5 Å[z]			7343	5474421	106.82	1.609	4.300	6.691	4.423		
2GTL, without linkers, anhydrous[%]		0	21060	2999510	116.51						
−, reduced, VS = 9.5 Å[x]			6459	2999608	116.50	1.635	5.704	7.529	5.802		
−, reduced, VS = 10.0 Å[x]			5694	2999607	116.50	1.637	5.684	7.509	5.786		
−, reduced, VS = 10.5 Å[x]			5164	2999607	116.50	1.637	5.684	7.509	5.789		
2GTL, without linkers, hydrated[y]	1.0	37748	58808	3924340	116.86						

Table 1 continued

Protein	f_K	N_w	N	V (Å^3)	R_G (Å)	$D \times 10^7$ (cm^2/s)	$[\eta]_{NVC}$ (cm^3/g)	$[\eta]_{FVC}$ (cm^3/g)	$[\eta]_{RVC}$ (cm^3/g)	$[\eta]_{CBS}$ (cm^3/g)	$[\eta]^a_{AVC}$ (cm^3/g)
−, reduced, VS = 9.5 Å[z]			9241	3926993	116.86	1.666[g]	5.958[g]	8.347[g]	6.071[g]		
−, reduced, VS = 10.0 Å[z]			8165	3926993	116.85	1.659[g]	5.972[g]	8.361[g]	6.091[g]		
−, reduced, VS = 10.5 Å[z]			7183	3926993	116.85	1.609	5.995	8.384	6.119		

f_K scaling factor acting on the hydration numbers, N_w number of water molecules, N number of beads, V total volume, R_G radius of gyration, D translational diffusion coefficient, $[\eta]$ intrinsic viscosity, *NVC* no volume correction, *FVC* full volume correction, *RVC* reduced volume correction, *CBS* cubic substitution, *AVC* adjusted volume correction, *BD* bead diameter, *ICOM* compression index, *VS* voxel size (edge length), *M* molar mass, d_{dot} dot density, r_{probe} radius of solvent probe, r_w radius of water molecule, V_w water volume, *IM-AT* initial model based on atoms or atomic groups, *IM-AM* initial model based on AA residues

[a] All values were computed by HYDRO++ (single-precision)

[b] $M = 5843$ g/mol, including Zn

[c] Hydration by HYDCRYST, based on $d_{dot} = 5$ Å^{-2}, $r_{probe} = r_w = 1.45$ Å, $V_w = 24.4$ Å^3

[d] $M = 6517.5$ g/mol

[e] $M = 13690$ g/mol

[f] Hydration by HYDCRYST, based on $d_{dot} = 3$ Å^{-2}, $r_{probe} = r_w = 1.50$ Å, $V_w = 27.0$ Å^3

[g] This value was computed in single-precision mode

[h] $M = 14313$ g/mol

[i] Hydration by HYDCRYST, based on $d_{dot} = 5$ Å^{-2}, $r_{probe} = r_w = 1.475$ Å, $V_w = 25.7$ Å^3

[j] $M = 76970$ g/mol

[k] $M = 76130$ g/mol

[l] $M = 76970$ g/mol; AA residues

[m] Hydration by HYDMODEL, based on $d_{dot} = 5$ Å^{-2}, $r_{probe} = r_w = 1.45$ Å, $V_w = 24.4$ Å^3

[n] $M = 76130$ g/mol; AA residues

[o] Initial model IM-AT of the capsid: each bead represents an atom or atomic group; $M = 2472.3$ kg/mol

[p] Reduction was performed by a running mean procedure, merging successive atoms or atomic groups of each chain of the trimeric building block into a single bead of given nominal diameter BD

[q] This is the maximum number of beads that can be handled by HYDRO in double-precision mode; further beads are ignored

[r] Reduction was performed by a running mean procedure, merging the atoms or atomic groups of ICOM successive AA residues of each chain of the trimeric building block into a single bead

[s] Initial model IM-AM of the capsid: each AA residue is represented by a single bead

[t] Reduction was performed by mapping the initial model IM-AM onto a hexagonal grid of given VS

[u] Hydration by HYDMODEL, based on $d_{dot} = 0.5$ Å^{-2}, $r_{probe} = r_w = 1.45$ Å, $V_w = 24.4$ Å^3

[v] Reduction was performed by mapping the hydrated initial model IM-AM onto a hexagonal grid of given VS

[w] All crystallographically observed AA residues (chains A–O) of the HBL complex and the 144 heme groups (attached to the globin chains A–L) are represented by single beads; $M = 3367.3$ kg/mol

[x] Reduction was performed by mapping the anhydrous model onto a hexagonal grid of given VS

[y] Hydration by HYDMODEL, based on $d_{dot} = 1$ Å^{-2}, $r_{probe} = r_w = 1.45$ Å, $V_w = 24.4$ Å^3

[z] Reduction was performed by mapping the hydrated model onto a hexagonal grid of given VS

[#] The original model of the HBL complex was modified by addition of 24 large beads representing the mass of AA residues missing in the terminal regions of the linker chains M–O; $M = 3448.6$ kg/mol

[%] The original model of the HBL complex was modified by omitting the beads representing the AA residues of the linker chains M–O; $M = 2475.0$ kg/mol

Table 2 Mean ratios of intrinsic viscosities [η] of anhydrous and hydrated protein models, obtained by various calculative approaches (preferentially in double-precision mode)

Protein	f_K	N	$\langle[\eta]_{NVC}/[\eta]_{RVC}\rangle$	$\langle[\eta]_{FVC}/[\eta]_{RVC}\rangle$	$\langle[\eta]_{CBS}/[\eta]_{RVC}\rangle$	$\langle[\eta]_{AVC}/[\eta]_{RVC}\rangle$[a]
4INS (chains A,B), anhydrous		404	0.906	1.601	0.989	1.097
−, hydrated	0.8–2.0	495–579	0.915 ± 0.003	1.605 ± 0.005	0.992 ± 0.003	1.066
4PTI, anhydrous		454	0.912	1.590	0.995	1.113
−, hydrated	0.8–2.0	554–656	0.920 ± 0.003	1.592 ± 0.005	0.995 ± 0.001	1.100 ± 0.003
1RBX, anhydrous		951	0.932	1.603	0.999	1.107
−, hydrated	0.8–1.5	1166–1261	0.937 ± 0.000	1.607 ± 0.006	0.992 ± 0.000[b]	1.115 ± 0.007
2LYZ, anhydrous		1001	0.929	1.639	0.988[b]	1.146
−, hydrated	0.8–2.0	1199–1341	0.938 ± 0.001	1.609 ± 0.007	0.992 ± 0.002[b]	1.145 ± 0.007
1P7T (mol. A), anhydrous		5414	0.965	1.629		
−, hydrated	1.0–7.0	6524–7236	0.965 ± 0.000	1.629 ± 0.008		
1P7T (mol. B), anhydrous		5358	0.964	1.587		
−, hydrated	1.0–7.0	6507–7202	0.965 ± 0.000	1.639 ± 0.009		
1P7T (mol. A), reduced, anhydrous		706	0.930	1.554	1.002	1.085
−, hydrated	1.0–7.0	1841–2385	0.950 ± 0.001	1.610 ± 0.011		1.193[c]
1P7T (mol. B), reduced, anhydrous		705	0.929	1.561	1.003	1.088
−, hydrated	1.0–7.0	1857–2417	0.949 ± 0.001	1.620 ± 0.012		1.196[c]
1FRS, anhydrous, reduced, BD = 9–24 Å		7722–540	0.971 ± 0.010	1.291 ± 0.008	1.027 ± 0.012[d]	1.104 ± 0.165[e]
−, ICOM = 3–48		7722–540	0.973 ± 0.006	1.285 ± 0.006	1.024 ± 0.006[f]	1.084 ± 0.117[g]
−, VS = 9–24 Å		7326–820	0.978 ± 0.007	1.275 ± 0.003	1.006 ± 0.003[h]	1.118 ± 0.097[i]
1FRS, hydrated, reduced, VS = 9–24 Å	1.0	10125–954	0.973 ± 0.008[j]	1.334 ± 0.007[j]	0.996 ± 0.005[h]	1.205 ± 0.167[i]
2GTL, original, anhydrous, reduced, VS = 10.5–11.5 Å		6939–5595	0.977 ± 0.001	1.402 ± 0.000		
2GTL, original, hydrated, reduced, VS = 10.5–11.5 Å	1.0	9072–7212	0.974 ± 0.001[k]	1.503 ± 0.003[k]		
2GTL, modified, anhydrous, reduced, VS = 10.5–11.5 Å		6958–5616	0.976 ± 0.001	1.411 ± 0.000		
2GTL, modified, hydrated, reduced, VS = 10.5–11.5 Å	1.0	9275–7343	0.973 ± 0.001[k]	1.516 ± 0.003[k]		
2GTL, without linkers, anhydrous, reduced, VS = 9.5–10.5 Å		6459–5164	0.982 ± 0.001	1.298 ± 0.000		

Table 2 continued

Protein	f_K	N	$\langle[\eta]_{NVC}/[\eta]_{RVC}\rangle$	$\langle[\eta]_{FVC}/[\eta]_{RVC}\rangle$	$\langle[\eta]_{CBS}/[\eta]_{RVC}\rangle$	$\langle[\eta]_{AVC}/[\eta]_{RVC}\rangle$[a]
2GTL, without linkers, hydrated, reduced, VS = 9.5–10.5 Å	1.0	9241–7183	0.981 ± 0.001[l]	1.373 ± 0.002[l]		

Abbreviations are explained in Table 1

[a] All values were computed from single-precision data

[b] This value was computed from single-precision data

[c] Single value for $f_K = 1.0$

[d] Calculated from the single and double-precision data for BD = 18–24 Å

[e] Calculated from the data for BD = 15–24 Å

[f] Calculated from the single and double-precision data for ICOM = 24–48

[g] Calculated from the data for ICOM = 12–48

[h] Calculated from the single-precision data for VS = 21–24 Å

[i] Calculated from the data for VS = 18–24 Å

[j] Calculated from the single and double-precision data for VS = 21–24 Å

[k] Calculated from the single and double-precision data for VS = 10.5–11.5 Å

[l] Calculated from the single and double-precision data for VS = 9.5–10.5 Å

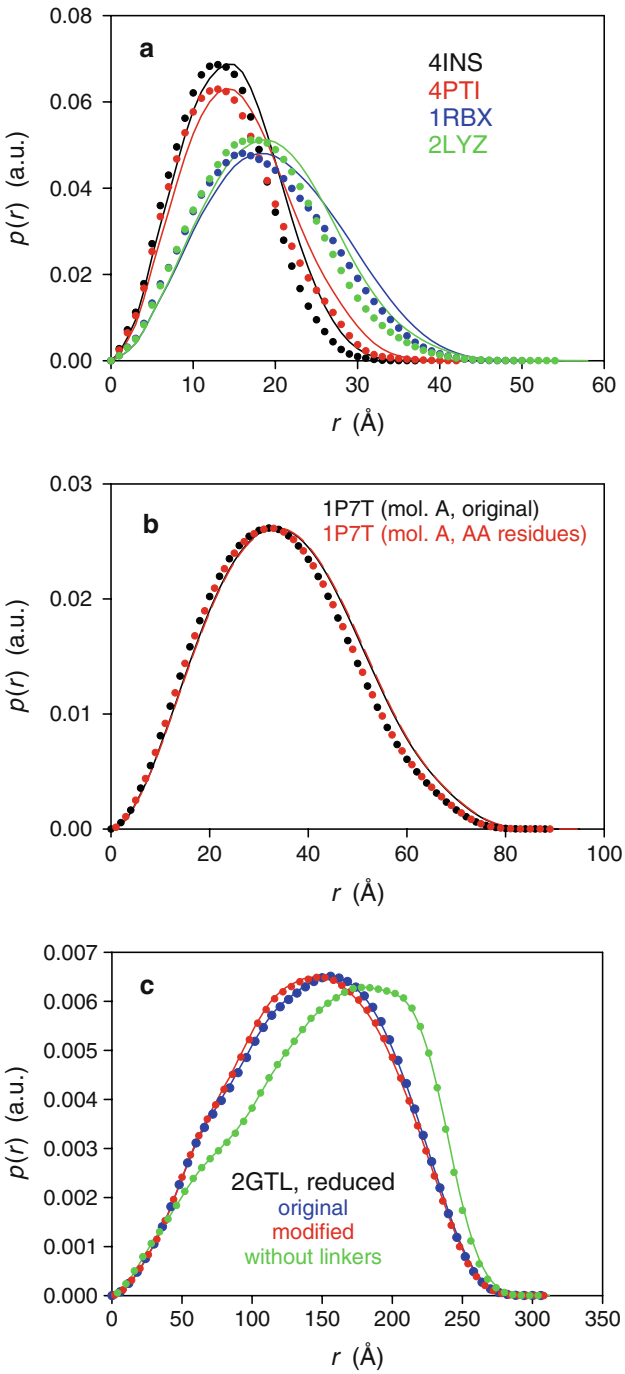

Fig. 4 Comparison of distance distribution functions $p(r)$ of selected space-filling multibead models for anhydrous and hydrated proteins: **a** insulin (*4INS*), pancreatic trypsin inhibitor (*4PTI*), ribonuclease A (*1RBX*), lysozyme (*2LYZ*), **b** malate synthase (1P7T, molecule A; original and reduced to AA residues), and **c** HBL complexes of *L.t.* hemoglobin (2GTL; reduced by means of the hexagonal grid approach, VS = 11 Å and 10 Å, respectively). The $p(r)$ functions referring to the anhydrous state (*circles*) are normalized to yield the same integral value (1.0); to match the height of these profiles, the functions for the hydrated state (*lines*) were rescaled appropriately. All hydrated models were generated with $f_K = 1.0$

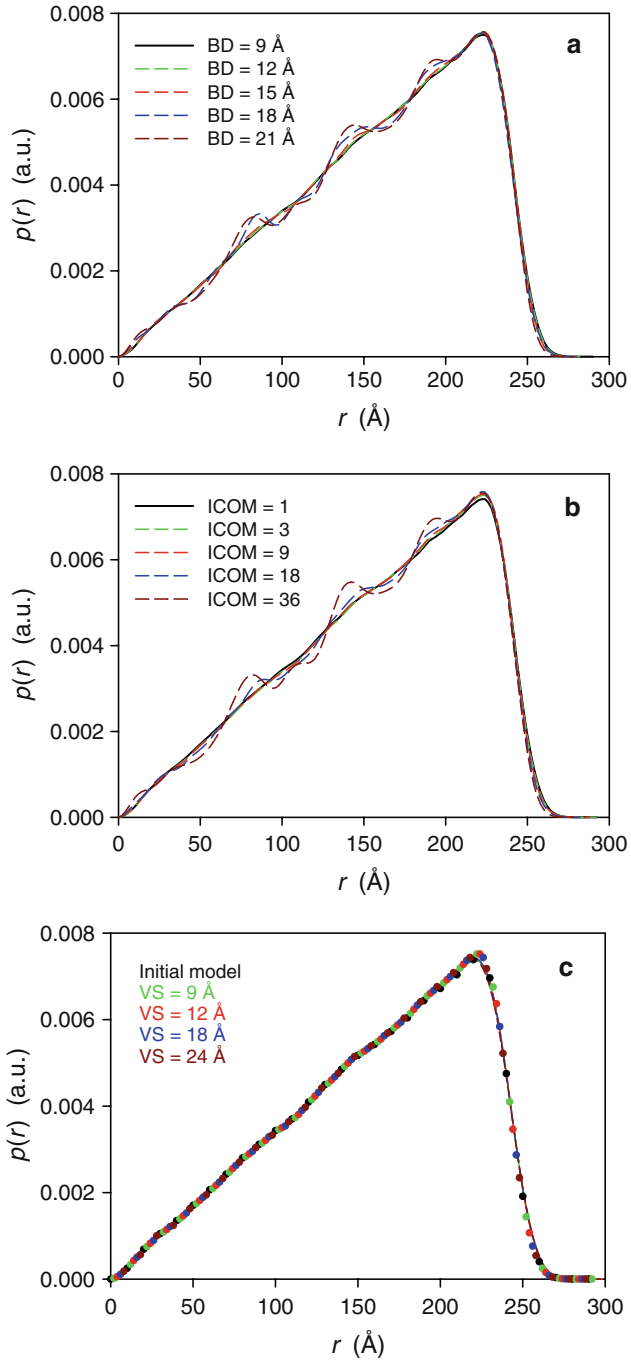

Fig. 5 Comparison of distance distribution functions $p(r)$ of selected reduced space-filling multibead models for the anhydrous (**a**–**c**) and hydrated (**c**) capsid of bacteriophage fr: **a** reduction of the crystal structures of the subunits by means of the running mean approach under variation of BD; **b** reduction of the crystal structures of the subunits by means of the running mean approach under variation of ICOM; **c** further reduction of the anhydrous capsid model (*circles*) obtained with ICOM = 1 (initial model IM-AM) or of the corresponding hydrated model (*lines*) by means of the hexagonal grid approach under variation of VS

corresponding to a distance slightly larger than the inner particle diameter (Glatter and Kratky 1982). The far-reaching agreement between the profiles obtained for different reduction approaches (RM, HG) and input parameters (BD, ICOM, VS), again, proves the validity of the applied computation procedures for the reduction process. As expected, the $p(r)$ functions of the grid models for the hydrated capsid are almost identical to the functions obtained for the anhydrous grid models. The wiggles observed in the $p(r)$ profiles of Fig. 5a and b are caused by the applied RM approach (generation of holes at the surface at high BD or ICOM values; cf. Fig. 2a, b), whereas use of the HG approach (Fig. 5c) results in rather smooth profiles (no holes at the surface over the whole range of VS values; cf. Fig. 2c).

Conclusions

In agreement with the results found for ellipsoid models of various axial ratios (Part 1), the RVC and CBS approaches for the prediction of intrinsic viscosities were successful. Application of our modified versions of HYDRO permit hydrodynamic model calculations in single-precision mode up to bead numbers N of about 11,000. However, a limitation of N of about 7,700 and computations in double-precision mode yield more accurate results for D. In the case of giant proteins composed of an immense number of atoms or constituents, both limits of N require preceding efficient reduction processes of the original models to be performed. Considering interactions of proteins occurring with the solvent water, modeling approaches for both anhydrous proteins and protein–water complexes have to be undertaken. Application of our hydration modeling strategies allow the generation of biophysically relevant protein–water models. Summarizing this modus operandi, realistic models of proteins can be generated. These models also take care of the fine details of the proteins under consideration. Prediction of structural and hydrodynamic parameters discloses the validity of the approaches applied.

When comparing the quality of hydrodynamic bead models, one has to discriminate between the appearance of the models, on the one hand, and the quality of the parameter predictions, on the other. Firstly, usage of our programs and approaches allows the precise construction of realistic protein models including preferentially bound water molecules, but requires usage of a multitude of beads (as many as possible). This proceeding is of importance for a strict comparison with the results of high-resolution techniques and many biological and presumable (bio)tech-

nological applications (Durchschlag et al. 2007; Durchschlag and Zipper 2008). Another aspect to be addressed is the accuracy of the parameter predictions. If in this case indeed usage of a multitude of beads is required remains to be established. In this context, a comparison of our respective results with the predictions obtained by other approaches such as SOMO (Rai et al. 2005), now incorporated in the program UltraScan (Demeler 2005), would be of high interest, in particular because SOMO also hydrates beads according to the amino acids they represent (by blowing up beads). A comparison of the models obtained by the approaches available and a critical assessment of the parameter predictions will be tackled in the near future.

Executable versions of our computer programs are available upon request; a suite of computer programs for bead reduction (programs PDB2AT, PDB2AM, MAP2GRID), hydration algorithms (program HYDCRYST including also essentials of HYDMODEL), and visualization tools (program HYD2PDBSCAL) will be deposited later on this year at the RASMB server.

Acknowledgments The authors are much obliged to J. García de la Torre for use of various versions of HYDRO, to Y.N. Vorobjev for SIMS, and to R.A. Sayle for RASMOL.

References

Berman HM, Westbrook J, Feng Z, Gilliland G, Bhat TN, Weissig H, Shindyalov IN, Bourne PE (2000) The protein data bank. Nucleic Acids Res 28:235–242. doi:10.1093/nar/28.1.235

Boeckmann B, Bairoch A, Apweiler R, Blatter M-C, Estreicher A, Gasteiger E, Martin MJ, Michoud K, O'Donovan C, Phan I, Pilbout S, Schneider M (2003) The SWISS-PROT protein knowledgebase and its supplement TrEMBL in 2003. Nucleic Acids Res 31:365–370. doi:10.1093/nar/gkg095

Byron O (1997) Construction of hydrodynamic bead models from high-resolution X-ray crystallographic or nuclear magnetic resonance data. Biophys J 72:408–415. doi:10.1016/S0006-3495(97)78681-8

Byron O (2008) Hydrodynamic modeling: the solution conformation of macromolecules and their complexes. Methods Cell Biol 84:327–373. doi:10.1016/S0091-679X(07)84012-X

Carrasco B, García de la Torre J (1999) Hydrodynamic properties of rigid particles: comparison of different modeling and computational procedures. Biophys J 76:3044–3057. doi:10.1016/S0006-3495(99)77457-6

Creighton TE (1993) Proteins: structures and molecular properties, 2nd edn. WH Freeman and Company, New York

Demeler B (2005) UltraScan—a comprehensive data analysis software package for analytical ultracentrifugation experiments. In: Scott DJ, Harding SE, Rowe AJ (eds) Analytical ultracentrifugation: techniques and methods. Royal Society of Chemistry, Cambridge, pp 210–230

Durchschlag H, Zipper P (2002) Modelling of protein hydration. J Phys Condens Matter 14:2439–2452. doi:10.1088/0953-8984/14/9/331

Durchschlag H, Zipper P (2005) Calculation of volume, surface, and hydration properties of biopolymers. In: Scott DJ, Harding SE, Rowe AJ (eds) Analytical ultracentrifugation: techniques and methods. Royal Society of Chemistry, Cambridge, pp 389–431

Durchschlag H, Zipper P (2008) Volume, surface and hydration properties of proteins. Prog Colloid Polym Sci 134:19–29

Durchschlag H, Zipper P, Wilfing R, Purr G (1991) Detection of small conformational changes of proteins by small-angle scattering. J Appl Crystallogr 24:822–831. doi:10.1107/S0021889891004831

Durchschlag H, Zipper P, Krebs A (2007) A comparison of protein models obtained by small-angle X-ray scattering and crystallography. J Appl Crystallogr 40:1123–1134. doi:10.1107/S0021889807045219

García de la Torre J, Navarro S, López Martínez MC, Díaz FG, López Cascales JJ (1994) HYDRO: a computer program for the prediction of hydrodynamic properties of macromolecules. Biophys J 67:530–531. doi:10.1016/S0006-3495(94)80512-0

García de la Torre J, Huertas ML, Carrasco B (2000) Calculation of hydrodynamic properties of globular proteins from their atomic-level structure. Biophys J 78:719–730. doi:10.1016/S0006-3495(00)76630-6

García de la Torre J, Del Rio Echenique G, Ortega A (2007) Improved calculation of rotational diffusion and intrinsic viscosity of bead models for macromolecules and nanoparticles. J Phys Chem B 111:955–961. doi:10.1021/jp0647941

Glatter O (1980) Computation of distance distribution functions and scattering functions of models for small angle scattering experiments. Acta Phys Austriaca 52:243–256

Glatter O, Kratky O (eds) (1982) Small angle X-ray scattering. Academic Press, London

Kuntz ID (1971) Hydration of macromolecules. III. Hydration of polypeptides. J Am Chem Soc 93:514–516. doi:10.1021/ja00731a036

Rai N, Nöllmann M, Spotorno B, Tassara G, Byron O, Rocco M (2005) SOMO (*SO*lution *MO*deler): differences between X-ray and NMR-derived bead models suggest a role for side chain flexibility in protein hydrodynamics. Structure 13:723–734 and supplemental data

Sayle RA, Milner-White EJ (1995) RASMOL: biomolecular graphics for all. Trends Biochem Sci 20:374–376. doi:10.1016/S0968-0004(00)89080-5

Serdyuk IN, Zaccai NR, Zaccai J (2007) Methods in molecular biophysics: structure, dynamics, function. Cambridge University Press, Cambridge

Svergun D, Barberato C, Koch MHJ (1995) *CRYSOL*—a program to evaluate X-ray solution scattering of biological macromolecules from atomic coordinates. J Appl Crystallogr 28:768–773. doi:10.1107/S0021889895007047

Vorobjev YN, Hermans J (1997) SIMS: computation of a smooth invariant molecular surface. Biophys J 73:722–732. doi:10.1016/S0006-3495(97)78105-0

Zipper P, Durchschlag H (2007a) Modelling of bacteriophage capsids and free nucleic acids. J Appl Crystallogr 40:s153–s158. doi:10.1107/S0021889807005936

Zipper P, Durchschlag H (2007b) Modeling complex biological macromolecules: reduction of multibead models. J Biol Phys 33:523–539. doi:10.1007/s10867-008-9063-6

Zipper P, Durchschlag H, Krebs A (2005) Modelling of biopolymers. In: Scott DJ, Harding SE, Rowe AJ (eds) Analytical ultracentrifugation: techniques and methods. Royal Society of Chemistry, Cambridge, pp 320–371